ChemComm

Accepted Manuscript

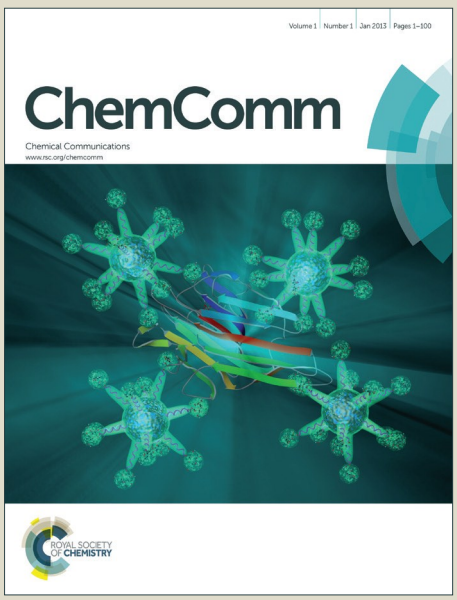

ROYAL SOCIETY OF CHEMISTRY

www.rsc.org/chemcomm

Cite this: DOI: 10.1039/c0xx00000x

www.rsc.org/xxxxxx

ARTICLE TYPE

Fluorescent and Photoconductive Nanoribbons as Dual-mode Sensor for Selective Discrimination of Alkyl Amines versus Aromatic Amines

Yibin Zhang, Cheng Peng, Xiaojie Ma, Yanke Che*, Jincai Zhao

Received (in XXX, XXX) Xth XXXXXXXXX 20XX, Accepted Xth XXXXXXXXX 20XX

DOI: 10.1039/b000000x

Highly fluorescent and photoconductive nanoribbons assembled from an asymmetric perylene diimide (PDI) were used as a dual-mode sensor for sensitive and selective discrimination of two classes of organic amines in the vapor phase, i.e., alkyl amines and aromatic amines.

Selective detection of trace amines in the vapor phase has attracted intense attention because of the increasing concerns in air pollution monitoring,[1-3] quality control of food,[4-6] and even medical diagnosis.[7, 8] Among the various detection technologies, fluorescent sensors[9, 10] and electronic sensors (e.g., chemiresistors)[1, 3, 6, 11] represent simple, cost-effective, and highly sensitive detection strategies. However, both electronic and fluorescent sensory materials reported thus far exhibit responses to all classes of amines (e.g., alkyl amines and aromatic amines), rather than a specific class. Although sensor arrays may provide selective discrimination among similar analytes,[12] multiple types of sensory materials (usually more than ten materials) and complicated analysis (e.g., PCA) are required. Therefore, simple and expedient detection technologies for selective discrimination of the types of amines are desirable, but still remain a big challenge.

In this work, we report that layered nanoribbons assembled from an asymmetric perylene diimide (molecule **1**, Figure 1b) simultaneously exhibit high photoconductivity and emission because of the large transversal molecular packing within the nanoribbon. We demonstrate that the nanoribbons can be used as a dual-mode sensor, which exhibited orthogonal responses (i.e., fluorescence quenching and photocurrent enhancement) when exposure to alkyl amines versus aromatic amines, thereby providing selective discrimination of alkyl amines versus aromatic amines. This dual-mode sensor may find the potential applications in bioanalytical chemistry for the discrimination of analytes that are present in multiple forms.

Synthesis of molecule **1** and self-assembly of **1** into nanoribbons were performed following previously reported procedure.[13] Transmission electron microscopy (TEM) reveals the formation of bundles of nanoribbons from molecule **1** with a high aspect ratio (Figure 1 and Figure S1). AFM imaging and line scanning further show the thinnest thickness of the isolated nanoribbon from **1** is about 6 nm (Figure 1c), which corresponds to the length of the two layers of molecule **1**. The resulting nanoribbons are highly emissive, as depicted in the fluorescence microscopy images (Figure 1b), which is consistent with the high fluorescence quantum yield (ca. 35 %).[13] Careful analysis of X-ray diffraction (XRD) patterns of the nanoribbons[14] confirms that molecule **1** adopts a slipping stacking with a substantial transversal offset within the nanoribbon. A transversal displacement of about 0.24 nm can be calculated based on 0.39 nm of π-stacking distance as observed in XRD result. Figure S2 shows the molecular packing that fits well the XRD patterns. Such a substantial transversal displacement would reduce the intermolecular interaction within the π-stack, thereby resulting in Frenkel exciton that dominates the emission and retains the dipole moment analogous to monomer.[15] The undisturbed transition dipole moment allows the efficient low energy excitonic transition and thus the efficient solid-state fluorescence as observed.

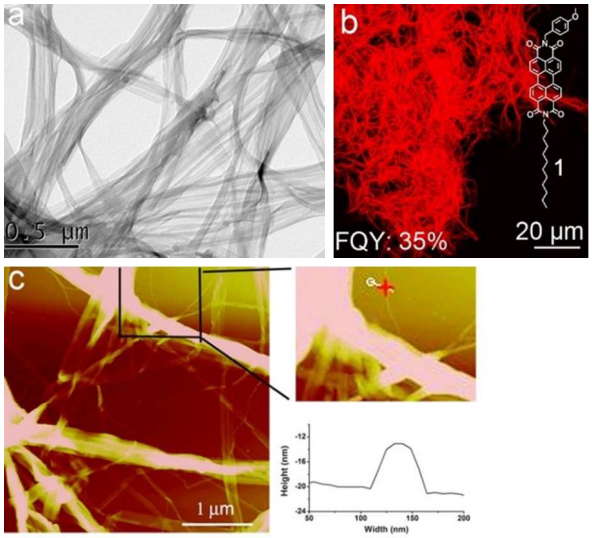

Figure 1. (a) TEM image of the nanoribbons assembled from **1**. (b) Fluorescence microscopy image of the nanoribbons assembled from **1.** (c) Tapping mode AFM and line scanning images of the nanoribbons from **1**.

Given the transversal molecular arrangement can create a slipped 2-D brickstone arrangement[16, 17] and thus increase the electronic communication between π-stacks, we envision that a net π-overlap enhancement may be achieved on the nanoribbon from **1** because the disadvantageous intra-π-stacked electronic coupling by the transversal molecular arrangement could be compensated. To corroborate this hypothesis, we investigated the

absorption and fluorescence spectra of the nanoribbons from **1**. As shown in Figure 2a, the absorption and fluorescence spectra of the nanoribbons are largely red-shifted compared to those of the individual molecule, indicative the large π-electron overlap within the nanoribbons.[18] Because the weak intermolecular interaction within the π-stack would result in the dipole moment analogous to the monomer and in turn the optical spectra analogous to the monomer, the observed large π-electron overlap within the nanoribbons must arise from the inter-π-stacked electronic overlap. The large π-electron coupling within the nanoribbons is also reflected by the efficient electron delocalization within the nanoribbons. Electron spin resonance (ESR) measurements of the sparse anionic radical within the nanoribbons that formed upon the partial reduction by hydrazine under argon show that an isotropic ESR signal with g = 2.0055 has the peak-to-peak line width of only 1.1 G (Figure 2b). This corresponds to electron hopping over twelve molecules (using the monomer radical with a width of 3.8 G for the calculation[19, 20]); this efficient electron delocalization indicates the strong π-electron coupling within the nanoribbon.

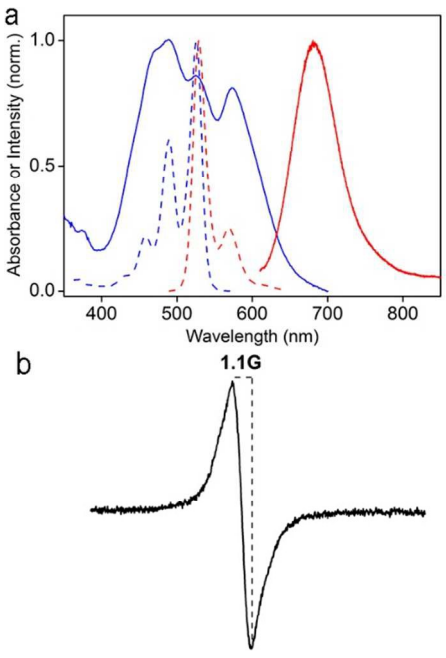

Figure 2. (a) Absorption (black) and fluorescence (red) spectra of molecular **1** in chloroform solution (dashed) and the nanoribbon state (solid). (b) ESR spectrum of the nanoribbons from **1** partially reduced by hydrazine vapor under argon.

Because that large π-overlap favors the stabilization of separated charge[21] as well as the electron delocalization,[22] a high photoconductivity is expected to be achieved over the nanoribbon from **1**. Indeed, as shown in Figure 3a, nanoribbons drop-cast onto the two-probe electrode exhibit remarkable photoconductivity upon white light irradiation (30 mW/cm^2), whereas the same nanoribbons are hardly conductive without light irradiation. For example, at an applied bias of 10 V, the photocurrent of 0.9±0.2 nA was observed when the nanoribbons from **1** were irradiated with white light (30 mW/cm^2) while the dark current is only 0.08±0.03 pA (Figure 3a). Such high photoconductivity over these nanoribbons is comparable to the nanomaterials consisting of molecularly connected electron donor and acceptor layers.[23, 24] Furthermore, as shown in Figure 3b, the photocurrent switching was demonstrated to be prompt and repeatable with the light on and off, indicating that the photoconductivity of the nanoribbons is very sensitive to the light.

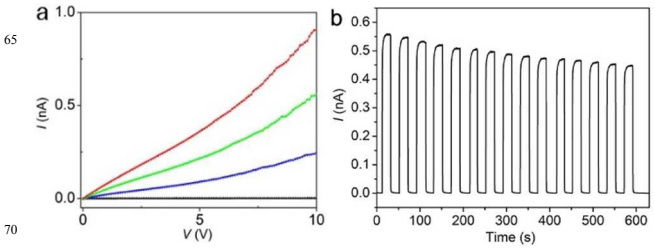

Figure 3. (a) I-V curves measured over the nanoribbon from **1** in the dark (black) and under white light irradiation of increasing power density (blue: 10, green: 20, red: 30 mW/cm^2). (b) Photocurrent (at an applied bias of 10 V) in response to turning on and off the irradiation (30 mW/mm^2).

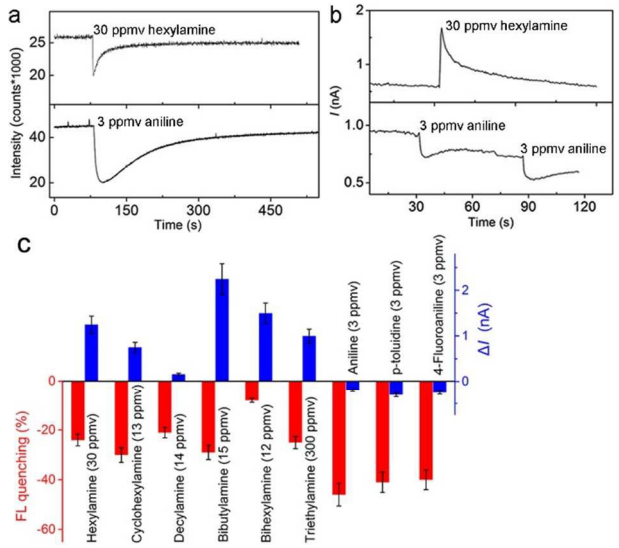

Figure 4. (a) Typical fluorescence quenching of the nanoribbons from **1** upon exposure to hexylamine (30 ppmv) and aniline (3 ppmv) vapors. (b) Typical photoconductive changes of the nanoribbons from **1** upon exposure to hexylamine (30 ppmv) and aniline (3 ppmv) vapors. (c) Columnar illustration of the orthogonal responses when exposed to alkyl amines versus aromatic amines.

The high fluorescence efficiency and high photoconductivity as above observed, together with the intrinsic high surface area and porosity in between piling nanoribbons upon deposition onto a substrate, motivated us to explore the dual-mode sensing performance of the nanoribbons, i.e., fluorescence and photoconductive responses upon exposure to the analytes. We chose two classes of amines, alkyl amines and aromatic amines, as the target analyses which have been widely used in various areas ranging from chemical to pharmaceutical industries.[1] Typically, upon exposure to hexylamine (30 ppmv) and aniline vapors (3 ppmv), remarkable fluorescence quenching of the nanoribbons drop-cast on the glass slice (the thickness of the nanoribbon film was determined by AFM; see Supplementary Information) was observed, due to electron transfer reactions between the n-type nanoribbons and reductive amines (as shown in Figure 4a). Surprisingly, hexylamine and aniline vapors resulted in contrary photoconductive changes, i.e., hexylamine

increased the photocurrent while aniline decreased the photocurrent. As shown in Figure 4b, the photocurrent of the nanoribbons increased from 0.7 nA to 1.7 nA when exposed to 30 ppmv vapor hexylamine, whereas the photocurrent decreased from 0.9 nA to 0.7 nA when exposed to 3 ppmv vapor aniline. Likewise, other alkyl amines, such as decylamine, cyclohexylamine, dibutylamine, dihexylamine, and trimethylamine, enhanced the photocurrent of nanoribbons. By contrast, the other aromatic amine, such as *p*-toluidine and 4-fluoaniline, decreased the photocurrent of nanoribbons (Figure 4c). The concentration-dependent responses in the fluorescence and photocurrent of the nanoribbons upon exposure to the amines were also monitored as displayed in Figures S3 and S4, indicating that both fluorescent and photoconductive responses are sensitive to the concentrations of amine vapors. The distinct photoconductive responses of alkyl amines vs. aromatic amines are likely related to the binding strength difference between the nanoribbons and amines. Because alkyl amines have relatively high oxidation potentials,[25, 26] the relatively weak electron donor-acceptor interaction between the nanoribbon and alkyl amines leads to a relative large separation distance; the photogenerated charge pair can easily escape from the Coulomb attraction to generate free charge[27] and thus increase the free charge carriers and in turn the photocurrent. In contrast, the aromatic amines have relative low oxidation potential,[25] and thus enables a stronger electron donor-acceptor interaction with the nanoribbon. This stronger interaction, together with π-π interaction can lead to the charge-transfer (CT) complex between molecule 1 and aromatic amines, which is hard to escape from the Coulomb attraction to generate free charge carriers. Furthermore, the CT complex can decrease the inherent photocurrent of the nanoribbons by trapping the photogenerated charge carriers on the pristine nanoribbons.[23] Obviously, compared to fluorescence quenching, the photocurrent changes are more sensitive to the subtle interactions between the sensory materials and the analytes that even resulted in opposite photoconductive changes. Importantly, these different transduction mechanisms allows the sensor to exhibit orthogonal responses when exposed to alkyl amines versus aromatic amines in the vapor phase (i.e., fluorescence quenching and photocurrent enhancement, Figure 4c), thereby providing an exquisite selectivity for the classes of amines as compared to the single-mode sensor, such as the individual fluorescence quenching sensor[9] or photoconductive sensor.[11, 24] In addition, for the photoconductive response, one advantage is that the signal amplification (i.e., sensitivity) can be easily accessible when using long interdigital electrodes instead of a simple electrode pair. Notably, when the mixture of a specific amine and other organic solvents or water vapor was blown onto the nanoribbons, the observed fluorescent and photoconductive responses are similar to those observed when only the amine vapor was blown onto the nanoribbons, indicative of the negligible effect of common matrix consisting of organic solvents and water. Of course, the photoconductivity of the nanoribbons is not very stable and further improvements on the photoconductive stability (e.g., via lowering the LUMO level of the building blocks by electron-withdrawing substituents) would be carried out towards better practical applications.

In conclusion, we report highly fluorescent and photoconductive nanoribbons assembled from an asymmetric PDI molecule were used as a dual-mode sensor for selective discrimination of two classes of organic amines in the vapor phase i.e., alkyl amines versus aromatic amines. This dual-mode sensor makes use of the different response mechanisms of fluorescence quenching and photoconductive changes to the classes of amines and exhibits orthogonal responses when exposed to alkyl amines versus aromatic amines, thereby providing an exquisite selectivity as compared to single-mode sensors. Further investigations of this approach in selective discrimination of subdivided classes of amines are currently underway in our laboratory.

This work was supported by NSFC (Nos. 21137004, 21221002, 21322701), the "Strategic Priority Research Program" of the Chinese Academy of Sciences (No. XDA09030200).

Notes and references

Key Laboratory of Photochemistry, Institute of Chemistry, Chinese Academy of Sciences, Beijing 100080, China. E-mail: ykche@iccas.ac.cn

† Electronic Supplementary Information (ESI) available: Details of the synthesis of molecules **1** and their self-assembly. AFM image and molecular packing within the nanoribbon. See DOI: 10.1039/b000000x/

1. T. Gao, E. S. Tillman and N. S. Lewis, *Chem. Mater.*, 2005, **17**, 2904-2911.
2. S. W. Thomas, III and T. M. Swager, *Adv. Mater.*, 2006, **18**, 1047-1050.
3. S. Rochat and T. M. Swager, *Angew. Chem., Int. Ed.*, 2014, **53**, 9792-9796.
4. M. T. Vecianangues, A. Marinefont and M. C. Vidalcarou, *J. Agric. Food Chem.*, 1997, **45**, 2036.
5. N. A. Rakow, A. Sen, M. C. Janzen, J. B. Ponder and K. S. Suslick, *Angew. Chem., Int. Ed.*, 2005, **44**, 4528-4532.
6. S. F. Liu, A. R. Petty, G. T. Sazama and T. M. Swager, *Angew. Chem., Int. Ed.*, 2015, **54**, 6554-6557.
7. H. Wolrath, R. Forsum, P. G. Larsson and H. Boren, *J. Clin. Microbiol.*, 2001, **39**, 4026.
8. G. Preti, J. N. Labows, J. G. Kostelc, S. Aldinger and R. Daniele, *J. Chromatogr. Biomed. Appl.*, 1988, **432**, 1.
9. Y. Che, X. Yang, S. Loser and L. Zang, *Nano Lett.*, 2008, **8**, 2219-2223.
10. Y. E, X. Ma, Y. Zhang, Y. Zhang, R. Duan, H. Ji, J. Li, Y. Che and J. Zhao, *Chem. Commun.* , 2014, **50**, 13596-13599
11. Y. Che, X. Yang, Z. Zhang, J. Zuo, J. S. Moore and L. Zang, *Chem. Commun.* , 2010, **46**, 4127-4129.
12. J. R. Askim, M. Mahmoudi and K. S. Suslick, *Chem. Soc. Rev.*, 2013, **42**, 8649-8682.
13. X. Liu, Y. Zhang, X. Pang, E. Yue, Y. Zhang, D. Yang, J. Tang, J. Li, Y. Che and J. Zhao, *J. Phys. Chem. C*, 2015, **119**, 6446-6452.
14. Y. Zhang, C. Peng, Z. Zhou, R. Duan, H. Ji, Y. Che and J. Zhao, *Adv. Mater.* , 2015, **27**, 320-325.
15. J. A. Schuller, S. Karaveli, T. Schiros, K. He, S. Yang, I. Kymissis, J. Shan and R. Zia, *Nature Nanotech.*, 2013, **8**, 271-276.
16. M. Gsaenger, J. H. Oh, M. Koenemann, H. W. Hoeffken, A.-M. Krause, Z. Bao and F. Wuerthner, *Angew. Chem. Int. Ed.*, 2010, **49**, 740-743.
17. M. M. Payne, S. R. Parkin, J. E. Anthony, C.-C. Kuo and T. N. Jackson, *J. Am. Chem. Soc.*, 2005, **127**, 4986-4987.
18. F. Wuerthner, T. E. Kaiser and C. R. Saha-Moeller, *Angew. Chem., Int. Ed.*, 2011, **50**, 3376-3410.
19. J. Baram, H. Weissman, Y. Tidhar, I. Pinkas and B. Rybtchinski, *Angew. Chem., Int. Ed.*, 2014, **53**, 4123-4126.
20. Y. Che, A. Datar, X. Yang, T. Naddo, J. Zhao and L. Zang, *J. Am. Chem. Soc.*, 2007, **129**, 6354-6355.
21. P. M. Kazmaier and R. Hoffmann, *J. Am. Chem. Soc.*, 1994, **116**, 9684-9691.
22. V. Coropceanu, J. Cornil, D. A. Da Silva Filho, Y. Olivier, R. Silbey and J.-L. Bredas, *Chem. Rev.*, 2007, **107**, 926-952.
23. Y. Yamamoto, T. Fukushima, Y. Suna, N. Ishii, A. Saeki, S. Seki, S. Tagawa, M. Taniguchi, T. Kawai and T. Aida, *Science*, 2006, **314**, 1761-1764.
24. Y. Che, X. Yang, G. Liu, C. Yu, H. Ji, J. Zuo, J. Zhao and L. Zang, *J. Am. Chem. Soc.*, 2010, **132**, 5743-5750.

25. M. A. Reppy, M. E. Cooper, J. L. Smithers and D. L. Gin, *J. Org. Chem.*, 1999, **64**, 4191-4195.
26. K. K. Barnes and C. K. Mann, *Anal. Chem.*, 1967, **32**, 1474-1479.
27. T. W. Holcombe, J. E. Norton, J. Rivnay, C. H. Woo, L. Goris, C. Piliego, G. Griffini, A. Sellinger, J.-L. Bredas, A. Salleo and J. M. J. Frechet, *J. Am. Chem. Soc.*, 2011, **133**, 12106-12114.